NASA TECHNICAL NOTE

NASA TN D-5702

C. 1

NASA TN D-5702

INVESTIGATION OF FATIGUE-CRACK GROWTH UNDER SIMPLE VARIABLE-AMPLITUDE LOADING

by C. Michael Hudson and K. N. Raju

Langley Research Center
Langley Station, Hampton, Va.

NATIONAL AERONAUTICS AND SPACE ADMINISTRATION • WASHINGTON, D. C. • MARCH 1970

1. Report No. NASA TN D-5702	2. Government Accession No.	3. Recipient's Catalog No.
4. Title and Subtitle INVESTIGATION OF FATIGUE-CRACK GROWTH UNDER SIMPLE VARIABLE-AMPLITUDE LOADING		5. Report Date March 1970 6. Performing Organization Code
7. Author(s) C. Michael Hudson and K. N. Raju		8. Performing Organization Report No. L-6834 10. Work Unit No. 126-14-15-01-23
9. Performing Organization Name and Address NASA Langley Research Center Hampton, Va. 23365		11. Contract or Grant No. 13. Type of Report and Period Covered Technical Note
12. Sponsoring Agency Name and Address National Aeronautics and Space Administration Washington, D.C. 20546		14. Sponsoring Agency Code

15. Supplementary Notes

16. Abstract

Variable-amplitude fatigue-crack-growth tests were conducted on simple sheet specimens made of 7075-T6 aluminum alloy. The numbers and the amplitudes of the high-load cycles applied in these tests were systematically varied to study their effects on subsequent low-load fatigue-crack growth.

The high-load cycles consistently delayed subsequent fatigue-crack growth at lower load levels. For a given low-load level, the higher the preceding high-load level was, the greater the delay in crack propagation. Furthermore, the delay in crack growth increased with increasing numbers of high-load cycles up to a limit. One high-load cycle caused approximately one-fourth of the maximum delay, and ten high-load cycles caused approximately one-half of the maximum delay. These delays probably resulted from residual compressive stresses generated in the material immediately ahead of the crack tip during the application of the high-load cycles.

17. Key Words Suggested by Author(s)	18. Distribution Statement
Fatigue-crack propagation Variable-amplitude loading 7075-T6 aluminum alloy Electron fractography	Unclassified – Unlimited

19. Security Classif. (of this report)	20. Security Classif. (of this page)	21. No. of Pages	22. Price*
Unclassified	Unclassified	22	$3.00

*For sale by the Clearinghouse for Federal Scientific and Technical Information Springfield, Virginia 22151

INVESTIGATION OF FATIGUE-CRACK GROWTH UNDER SIMPLE VARIABLE-AMPLITUDE LOADING

By C. Michael Hudson and K. N. Raju
Langley Research Center

SUMMARY

Variable-amplitude fatigue-crack-growth tests were conducted on simple sheet specimens made of 7075-T6 aluminum alloy. The numbers and the amplitudes of the high-load cycles applied in these tests were systematically varied to study their effects on subsequent low-load fatigue-crack growth.

The high-load cycles consistently delayed subsequent fatigue-crack growth at lower load levels. For a given low-load level, the higher the preceding high-load level was, the greater the delay in crack propagation. Furthermore, the delay in crack growth increased with increasing numbers of high-load cycles up to a limit. One high-load cycle caused approximately one-fourth of the maximum delay, and ten high-load cycles caused approximately one-half of the maximum delay. These delays probably resulted from residual compressive stresses generated in the material immediately ahead of the crack tip during the application of the high-load cycles.

Electron fractographic studies showed that at a given stress level, fatigue cracks propagated more slowly immediately after the application of a high-load cycle than they did immediately before its application. This lower crack-growth rate is consistent with the delay in crack growth observed on the macroscopic level.

INTRODUCTION

Fatigue cracks sometimes are initiated quite early in the life of aircraft structures. (See ref. 1, for example.) In order to predict the fatigue behavior of such structures, it is necessary to understand how these cracks propagate. Many theoretical and experimental investigations have been conducted to date in an effort to develop this understanding. Most of these investigations have dealt with constant-amplitude loading conditions, and several have led to analysis procedures which satisfactorily correlate data generated under such conditions. (The stress intensity analysis, applied to the fatigue-crack-growth phenomena by Paris (ref. 2) and the notch analysis developed by McEvily and Illg (ref. 3) are two examples.) However, aircraft structures experience random loadings in which high-amplitude load cycles are frequently followed by load cycles of lower amplitude. Under

such loading sequences, fatigue-crack-growth rates at the lower amplitudes are lower than they would be under constant-amplitude conditions. (See refs. 4 and 5.) Consequently, prediction of crack growth at these lower stress levels may be erroneous if the calculations are based on constant-amplitude data.

An experimental study (reported herein) has been conducted as a step toward understanding the effects of infrequent high loads on subsequent crack growth. Axial-load fatigue-crack-growth tests were conducted on 7075-T6 aluminum alloy specimens. The number of cycles at a given loading level and the amplitudes of the applied loadings were systematically varied in these tests to determine their influence on subsequent fatigue-crack growth. In addition, a fractographic analysis was performed on a representative specimen in an electron microscope.

SYMBOLS

The units used for physical quantities defined in this paper are given in both U.S. Customary Units and in the International System of Units (SI). (See ref. 6.) Factors relating these two systems of units are given in an appendix.

a	one-half of total length of a central symmetrical crack, in. (cm)
K_H	theoretical stress-concentration factor for a circular hole
K_N	theoretical stress-concentration factor for a crack, $1 + \frac{1}{2}\left(K_H - 1\right)\sqrt{\frac{a}{\rho_e}}$
N	number of cycles
P	maximum applied load, lbf (newton)
R	ratio of minimum stress to maximum stress
S_g	gross stress, P/wt, ksi $\left(N/m^2\right)$
S_{net}	instantaneous net section stress, $\frac{P}{t(w - 2a)}$, ksi $\left(N/m^2\right)$
t	specimen thickness, in. (mm)
w	specimen width, in. (mm)

ρ_e effective radius of curvature at the tip of a fatigue crack (equals 0.002 in. (51 μm) for 7075-T6 aluminum alloy (see ref. 3))

EXPERIMENTAL AND ANALYTICAL PROCEDURES

Specimens

The material was taken from the special stock of 0.090 in. (2.28 mm) thick 7075-T6 aluminum alloy described in reference 7 and retained at Langley Research Center for fatigue experiments. Tensile properties of this material (table I) were obtained by using standard ASTM tensile specimens.

Sheet specimens 2 in. (51 mm) wide and $12\frac{5}{8}$ in. (321 mm) long were used in all fatigue tests. (See fig. 1.) A crack starter notch 0.10 in. (2.54 mm) long by 0.01 in. (0.25 mm) wide was cut into the center of each of these specimens by using an electrical discharge process. All specimens were made with the longitudinal axis of the specimens parallel to the rolling direction of the sheet.

A set of reference lines (ref. 8) was photographically printed on the surface of the specimens to mark intervals in the path of the crack. Metallographic examination and tensile tests conducted on specimens bearing reference lines indicated that the lines had no observable effect on the material.

Tests

Constant and variable-amplitude fatigue-crack-growth tests were conducted under axial loading conditions. The stress ratio (ratio of the minimum applied stress to the maximum applied stress) was approximately zero in these tests. The constant-amplitude tests were conducted to provide baseline data. In the variable-amplitude tests, a crack was generally initiated and propagated to a half-length of 0.25 in. (6.4 mm) at a low-load level. One or more high-load cycles were then applied, followed by a subsequent series of low-load cycles to failure. The individual test programs are described in detail in the section "Results and Discussion."

A hydraulic axial-load fatigue-testing machine (ref. 9) was used in this investigation. This machine had a load capacity of ±20 000 lbf (±89 kN) and an operating frequency of 900 cpm (15 Hz). Loads were continuously monitored by measuring the output of a strain-gage dynamometer in series with the specimens. The maximum error in loading was ±1 percent of the applied load.

Fatigue-crack growth was observed through 10-power microscopes while the specimen was illuminated with stroboscopic light. The number of cycles required to propagate the crack to each reference line was recorded.

The effects of the high-load cycles on fatigue-crack growth at the subsequent low-load level were determined by comparing the data from the variable-amplitude tests with the baseline data from the constant-amplitude tests. This comparison was made by taking the difference between (a) the number of subsequent low-load cycles required to propagate the crack to failure, and (b) the number of equivalent load cycles required to propagate a crack of equal length to failure in a constant-amplitude test. The difference between these two numbers of cycles is the delay in crack propagation resulting from the application of the high-load cycle(s).

The fracture surface of one of the specimens tested in this investigation was studied with an electron microscope. Two-stage carbon replicas were chromium-shadowed at an angle of 45^{o}, and were observed under an electron microscope at a magnification of $\times$ 11 000. Two regions on the fracture surface were studied: (a) the region which was fatigue-cracked immediately before the application of a high-load cycle, and (b) the region which was fatigue-cracked immediately after the application of this high-load cycle. The results of this fractographic study were compared with the macroscopically observed behavior of the fatigue crack before and after the application of this high-loading cycle.

Analysis Procedure

Fatigue-crack propagation is generally understood to be controlled by the stress conditions in the vicinity of the crack tip. McEvily and Illg (ref. 3) proposed that these stress conditions can be characterized by the product of the theoretical stress-concentration factor for the crack K_N and the instantaneous net section stress, S_{net}, where

$$K_N = 1 + \frac{1}{2}\left(K_H - 1\right)\sqrt{\frac{a}{\rho_e}} \tag{1}$$

and

$$S_{net} = \frac{P}{t(w - 2a)} \tag{2}$$

The parameter ρ_e is the effective radius of curvature at the tip of the fatigue crack. This parameter was found (ref. 3) to have a value of 0.002 in. (51 μm) for 7075-T6 aluminum alloy. The term K_H is the theoretical stress-concentration factor for a circular hole. A plot of K_N against $2a/w$ for the specimens tested is shown in figure 2.

McEvily and Illg successfully correlated fatigue-crack-growth rates with $K_N S_{net}$ in reference 3. One of the materials for which rates were successfully correlated was

7075-T6 aluminum alloy tested at a stress ratio R of zero. Since the same material and loading conditions were used in the present investigation, $K_N S_{net}$ was used for analysis herein.

RESULTS AND DISCUSSION

Fatigue Tests

Test series I.- Experiments were conducted to study the effect of single high-load cycles on subsequent crack growth at a low-load level. The test specimens were subjected to the loading program shown in sketch 1.

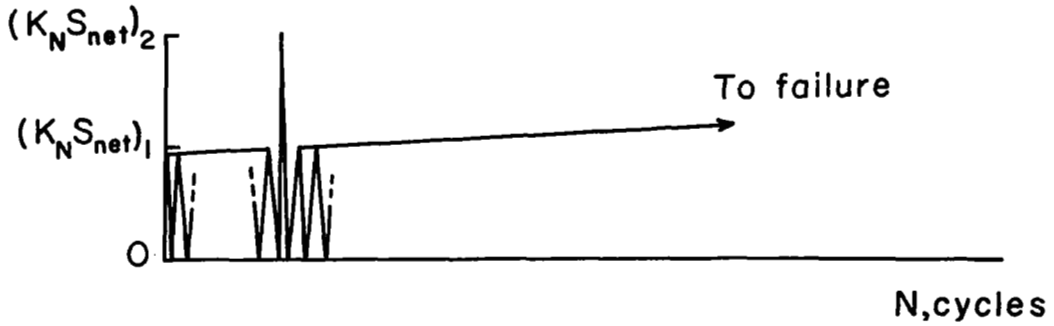

Sketch 1

A fatigue crack was initiated and propagated in each specimen to a half-length of 0.25 in. (6.4 mm) at a load level producing a $(K_N S_{net})_1$ when the 0.25-in. (6.4-mm) half-length was reached. A single high-load cycle producing a $(K_N S_{net})_2$ at the crack tip was then applied. The specimens were then cycled to failure at a load level again producing $(K_N S_{net})_1$ at the tip of the crack. The values of $K_N S_{net}$ applied in each test and of the corresponding values of gross stress S_g are listed in the following table:

Test	$(K_N S_{net})_1$		$(S_g)_1$		$(K_N S_{net})_2$		$(S_g)_2$	
	ksi	GN/m^2	ksi	MN/m^2	ksi	GN/m^2	ksi	MN/m^2
1	375	2.59	31.25	215	450	3.10	37.50	259
2	300	2.07	25.00	172	450	3.10	37.50	259
3	225	1.55	18.75	129	450	3.10	37.50	259
4	300	2.07	25.00	172	375	2.59	31.25	215
5	225	1.55	18.75	129	375	2.59	31.25	215
6	150	1.03	12.50	86	375	2.59	31.25	215
7	225	1.55	18.75	129	300	2.07	25.00	172
8	150	1.03	12.50	86	300	2.07	25.00	172
9	150	1.03	12.50	86	225	1.55	18.75	129

The delay in crack propagation resulting from each high load is plotted against $(K_N S_{net})_1$ in figure 3. This figure shows that for a given value of $(K_N S_{net})_1$, the higher the value of $(K_N S_{net})_2$, the greater was the delay in propagation.

Test series II.- Several specimens were subjected to the loading program shown in sketch 2 to study the delay in crack growth resulting from the application of a large number of high-load cycles.

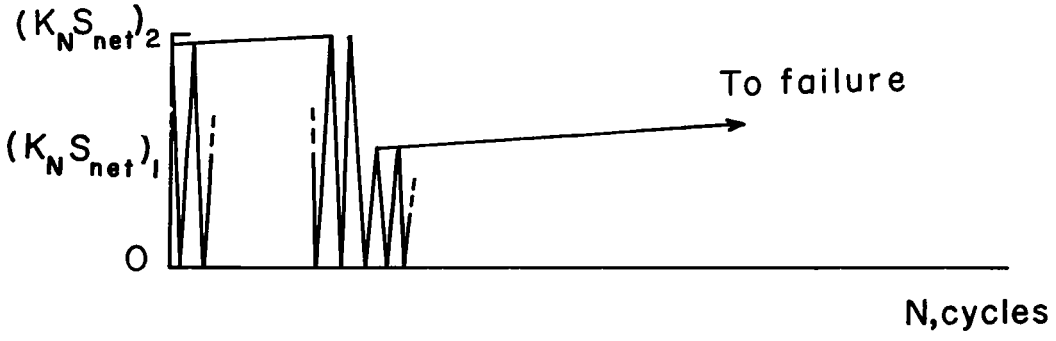

Sketch 2

A fatigue crack was initiated and propagated in each specimen to a half-length of 0.25 in. (6.4 mm) at a high-load level producing $(K_N S_{net})_2$ when the 0.25-in. (6.4-mm) half-length was reached. The load level was then dropped to a level producing $(K_N S_{net})_1$ and the specimen was cycled to failure. The same values of $(K_N S_{net})_1$ and $(K_N S_{net})_2$ were applied in this test series and in test series I to make the results comparable.

The plot of delay in propagation against $(K_N S_{net})_1$ is shown in figure 4. As in test series I, the higher the value of $(K_N S_{net})_2$, the greater was the subsequent delay in propagation for a given value of $(K_N S_{net})_1$.

Comparison of the results from this test series with the results from test series I (fig. 5) showed that the delay in propagation was greater for specimens subjected to a large number of high-load cycles than in specimens subjected to a single high-load cycle.

Test series III.- A number of specimens were tested to provide a more definitive evaluation of the effects of different numbers of high-load cycles on subsequent fatigue-crack growth at a lower load level. These specimens were subjected to the loading program shown in sketch 3.

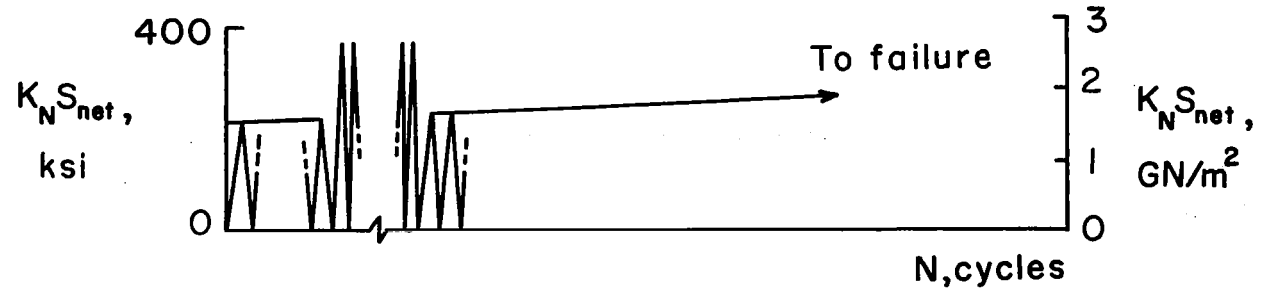

Sketch 3

A fatigue crack was initiated and propagated in each specimen to a half-length of 0.25 in. (6.4 mm) at a load level producing a $K_N S_{net}$ of 225 ksi $(1.55\ GN/m^2)$ when the 0.25-in. (6.4-mm) half-length was reached. A number of high-load cycles, each producing a $K_N S_{net}$ of 375 ksi $(2.59\ GN/m^2)$, were then applied. (The fatigue cracks did not propagate a significant amount as a result of these high-load cycles.) The specimens were then cycled to failure at the original low-load level.

The number of specimens tested in this series and the number of high-load cycles applied to each specimen are as follows:

Number of specimens tested	Number of high-load cycles applied
3	1
2	5
1	10
1	20
1	28

The result from one experiment in test series II was also applicable to this test series.

The delays in crack growth resulting from the different numbers of high-load cycles are plotted against the number of high-load cycles in figure 6. The vertical line in figure 6 represents a limiting delay (6000 cycles) for the 375 to 225 ksi $(2.59$ to $1.55\ GN/m^2)$ loading sequence. This limiting delay occurred in a test in series II where the crack was initiated and propagated to a half-length of 0.25 in. (6.4 mm) at the high-load level and then cycled to failure at the low-load level.

One high-load cycle caused approximately one-fourth of the maximum delay found for the loading sequence used, and ten high-load cycles caused approximately one-half of the maximum delay.

Test series IV.- Specimens were tested to study whether the fatigue loading applied before the application of a single high-load cycle affected fatigue-crack growth at a subsequent low-load level. One of the four loading programs shown in sketch 4 was used in each test.

A fatigue crack was initiated and propagated in each specimen to a half-length of 0.25 in. (6.4 mm) at a load level producing $(K_N S_{net})_3$ when the 0.25-in. (6.4-mm) half-length was reached. A single high-load cycle producing a $(K_N S_{net})_2$ of 375 ksi $(2.59\ GN/m^2)$ was then applied. The specimens were then cycled to failure at a load level producing a $(K_N S_{net})_1$ of 150 ksi $(1.03\ GN/m^2)$. The values of the $(K_N S_{net})_3$ applied in each test, the corresponding $(S_g)_3$ and the numbers of specimens tested were:

Loading program shown in schematic	Number of specimens tested	$(K_N S_{net})_3$		$(S_g)_3$	
		ksi	GN/m^2	ksi	MN/m^2
4(a)	1	150	1.03	12.50	86
4(b)	3	225	1.55	18.75	129
4(c)	2	300	2.07	25.00	172
4(d)	1	375	2.59	31.25	215

Because the values of $(K_N S_{net})_1$ and $(K_N S_{net})_2$ are the same for each loading program in this test series, any differences between the delay in propagation for the four programs would result principally from the differences in the values of $(K_N S_{net})_3$. A plot of delay in propagation against $(K_N S_{net})_3$ is shown in figure 7. Included in this figure are data points from test series I and II which are directly applicable to test series IV. The delay in propagation progressively increased with increasing $(K_N S_{net})_3$; thus the fatigue loading applied before the application of a single high-load cycle can significantly retard fatigue-crack growth at a subsequent low-load level.

The Role of Residual Stress

The delays in crack growth found in test series I to IV probably resulted from the residual compressive stresses left in the material immediately ahead of the crack tip after the application of the high-load cycles. A description of the generation of these residual stresses at crack tips is given in reference 10. This residual compressive stress could delay fatigue-crack growth at the low-load levels by reducing the magnitude of the tensile stress acting at the crack tip.

Fractographic Examination

Typical electron micrographs of the fracture surface of a specimen tested in test series I are shown in figure 8. The values of $K_N S_{net}$ for the high-load and low-load

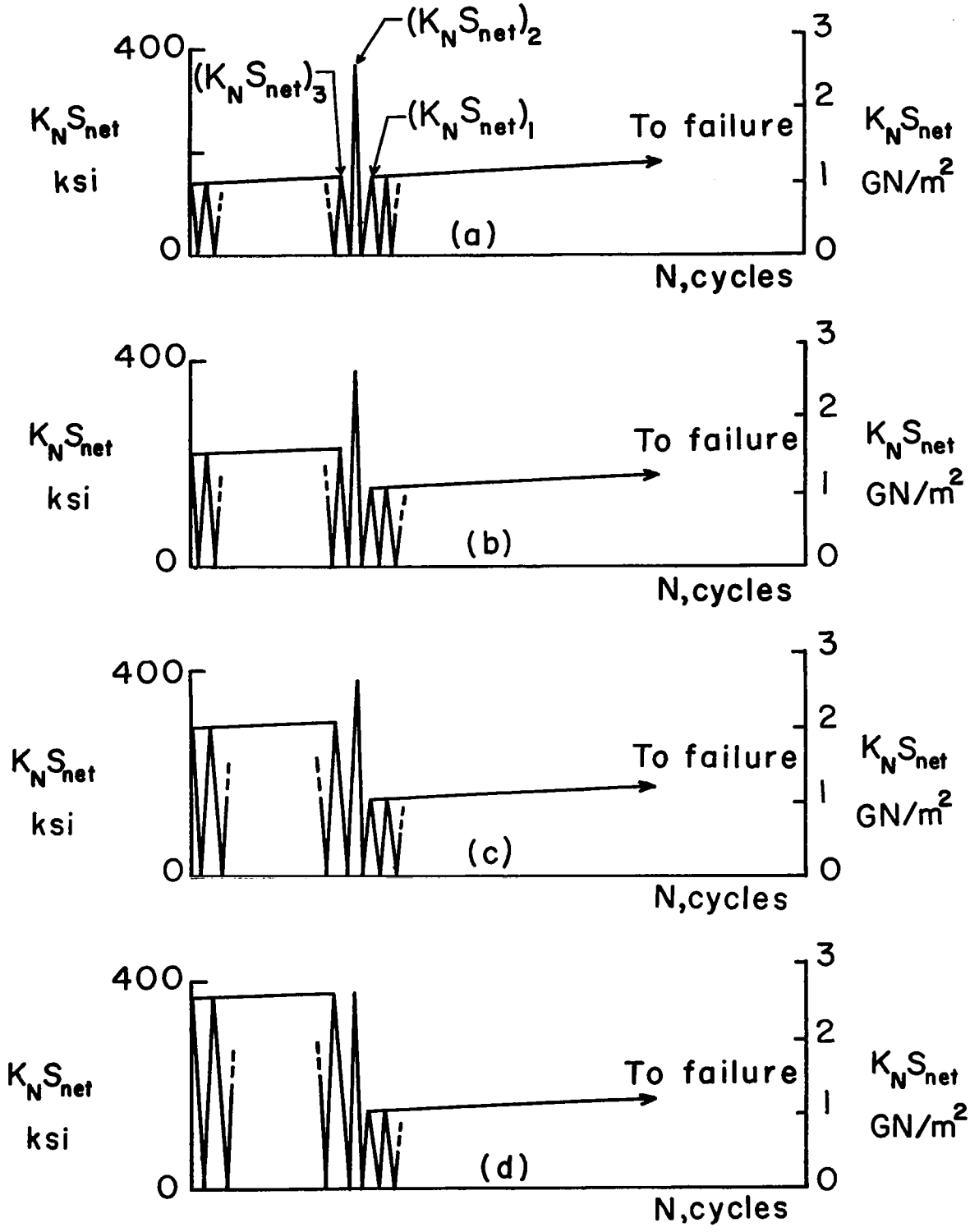
400
0
$K_N S_{net}$ ksi
$(K_N S_{net})_3$
$(K_N S_{net})_2$
$(K_N S_{net})_1$
To failure
(a)
N,cycles
3
2
1
0
$K_N S_{net}$ GN/m²
(b)
(c)
(d)

Sketch 4

cycles were 375 and 150 ksi (2.59 and 1.03 GN/m^2), respectively. Figure 8(a) shows the region created by low-load cycles applied immediately before the high-load cycle. Widely spaced, rather discontinuous striations occurred in this region. Figure 8(b) shows the region created by identical low-load cycles applied immediately after the high-load cycle. The resulting striations are much more closely spaced than the striations in figure 8(a), and thus indicate a much lower fatigue-crack-growth rate. This lower rate is consistent with the apparent delay in crack growth observed.

CONCLUSIONS

A series of constant and variable-amplitude fatigue-crack growth tests was conducted on sheet specimens made of 7075-T6 aluminum alloy. The numbers and the amplitudes of the high-load cycles applied in the variable-amplitude tests were systematically varied to study their effects on subsequent low-load crack growth. These effects were determined by comparing low-load crack-growth behavior with the crack-growth behavior in the constant-amplitude tests. Electron fractographs were taken to compare the macroscopic and microscopic fatigue-crack-growth behaviors. Analysis of the test results supports the following conclusions:

1. The application of high-load cycles consistently delayed subsequent fatigue-crack growth at lower load levels.

2. The delay in crack growth increased with increasing numbers of high-load cycles up to a limiting value. One high-load cycle caused approximately one-fourth of the maximum delay, and ten high-load cycles caused approximately one-half of the maximum delay.

3. For a given low-load level, the higher the preceding high-load level, the greater was the delay in crack propagation.

4. For a three-level loading sequence (that is, multiple intermediate load to single high load to multiple low load) the higher the intermediate-load level, the greater was the delay in crack growth at the low-load level.

5. Electron fractographic studies of one of the fractured specimens showed that at a given stress level, fatigue cracks propagated more slowly immediately after the application of a high-load cycle than immediately before its application. This retardation is consistent with the delay in crack growth observed on the macroscopic level.

6. Generally, the delays observed in these tests were attributed to residual compressive stresses produced during previously applied high-load cycles.

Langley Research Center,
National Aeronautics and Space Administration,
Langley Station, Hampton, Va., January 9, 1970.

APPENDIX

CONVERSION OF U.S. CUSTOMARY UNITS TO SI UNITS

The International System of Units (SI, ref. 6) was adopted by the Eleventh General Conference of Weights and Measures, Paris, October, 1960, in Resolution No. 12. Conversion factors for the units used herein are given in the following table:

To convert from U.S. Customary Units	Multiply by –	To obtain SI Units
lbf	4.448222	newton (N)
in.	2.54×10^{-2}	meter (m)
ksi	6.894757×10^{6}	newtons/meter^2 (N/m^2)
cpm	1.67×10^{-2}	hertz (Hz)

Prefixes and symbols to indicate multiples of units are as follows:

Multiple	Prefix	Symbol
10^{-6}	micro	μ
10^{-3}	milli	m
10^{-2}	centi	c
10^{3}	kilo	k
10^{6}	mega	M
10^{9}	giga	G

REFERENCES

1. Castle, Claude B.; and Ward, John F.: Fatigue Investigation of Full-Scale Wing Panels of 7075 Aluminum Alloy. NASA TN D-635, 1961.

2. Paris, Paul C.: The Fracture Mechanics Approach to Fatigue. Fatigue – An Interdisciplinary Approach, John J. Burke, Norman L. Reed, and Volker Weiss, eds., Syracuse Univ. Press, 1964, pp. 107-132.

3. McEvily, Arthur J., Jr.; and Illg, Walter: The Rate of Fatigue-Crack Propagation in Two Aluminum Alloys. NACA TN 4394, 1958.

4. Hudson, C. Michael; and Hardrath, Herbert F.: Effects of Changing Stress Amplitude on the Rate of Fatigue-Crack Propagation in Two Aluminum Alloys. NASA TN D-960, 1961.

5. Schijve, J.: Fatigue Crack Propagation in Light Alloy Sheet Material and Structures. Rep. MP.195, Nationaal Luchtvaartlaboratorium (Amsterdam), Aug. 1960.

6. Comm. on Metric Pract.: ASTM Metric Practice Guide. NBS Handbook 102, U.S. Dep. Com., Mar. 10, 1967.

7. Grover, H. J.; Hyler, W. S.; Kuhn, Paul; Landers, Charles B.; and Howell, F. M.: Axial-Load Fatigue Properties of 24S-T and 75S-T Aluminum Alloy as Determined in Several Laboratories. NACA Rep. 1190, 1954. (Supersedes NACA TN 2928.)

8. Hudson, C. Michael: Fatigue-Crack Propagation in Several Titanium and Stainless Steel Alloys and One Superalloy. NASA TN D-2331, 1964.

9. Imig, L. A.: Effect of Initial Loads and of Moderately Elevated Temperature on the Room-Temperature Fatigue Life of Ti-8Al-1Mo-1V Titanium-Alloy Sheet. NASA TN D-4061, 1967.

10. Hudson, C. Michael; and Hardrath, Herbert F.: Investigation of the Effects of Variable-Amplitude Loadings on Fatigue Crack Propagation Patterns. NASA TN D-1803, 1963.

TABLE I.- AVERAGE TENSILE PROPERTIES OF 7075-T6 ALUMINUM ALLOY

Ultimate tensile strength		Yield stress (0.2-percent offset)		Young's modulus of elasticity		Elongation in 2-in. (51-mm) gage length, percent	No. of tests
ksi	MN/m^2	ksi	MN/m^2	ksi	GN/m^2		
83.2	574	75.9	523	10 100	69.6	12	20

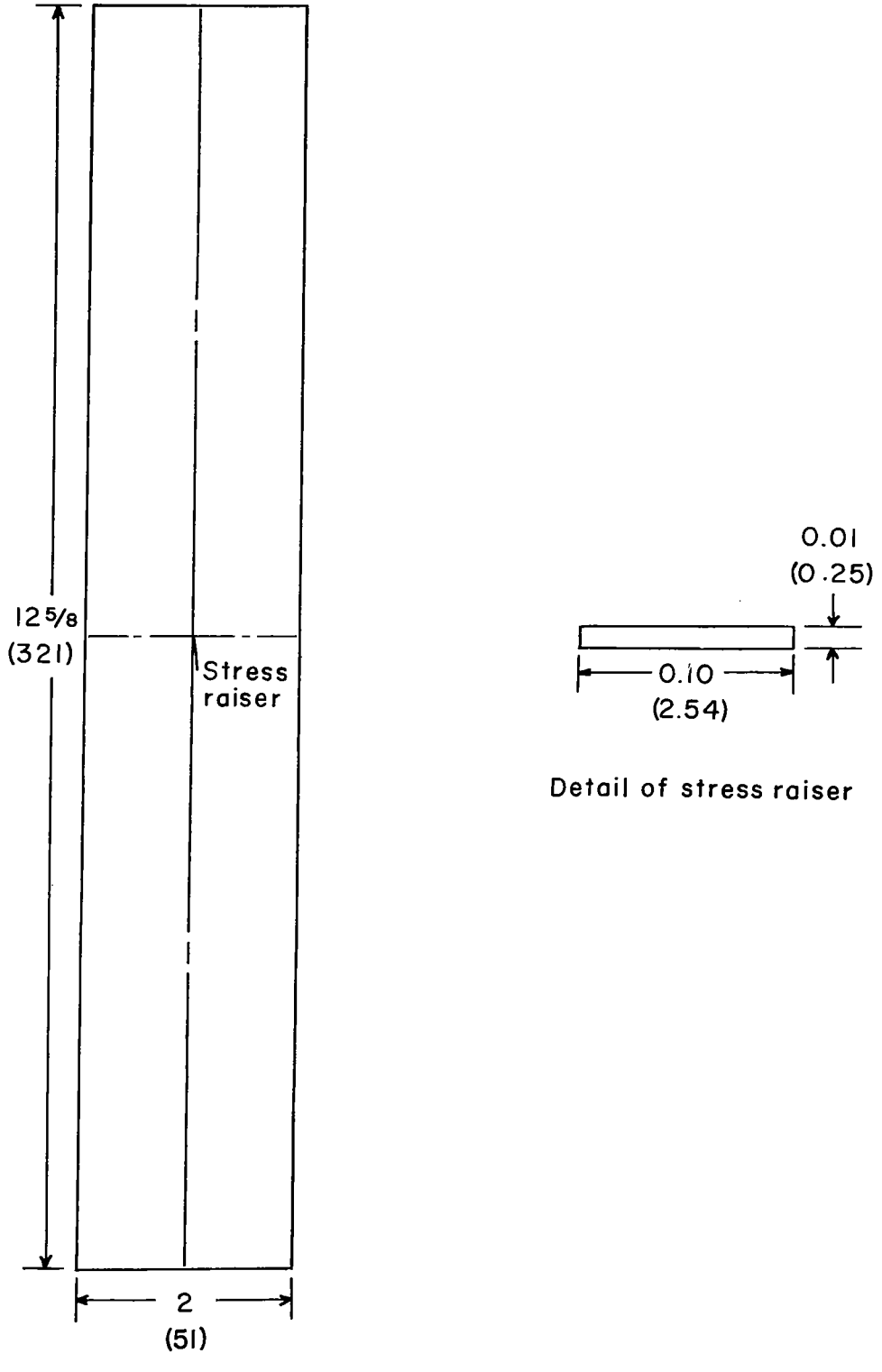

Figure 1.- Specimen configuration. All dimensions are in inches (mm).

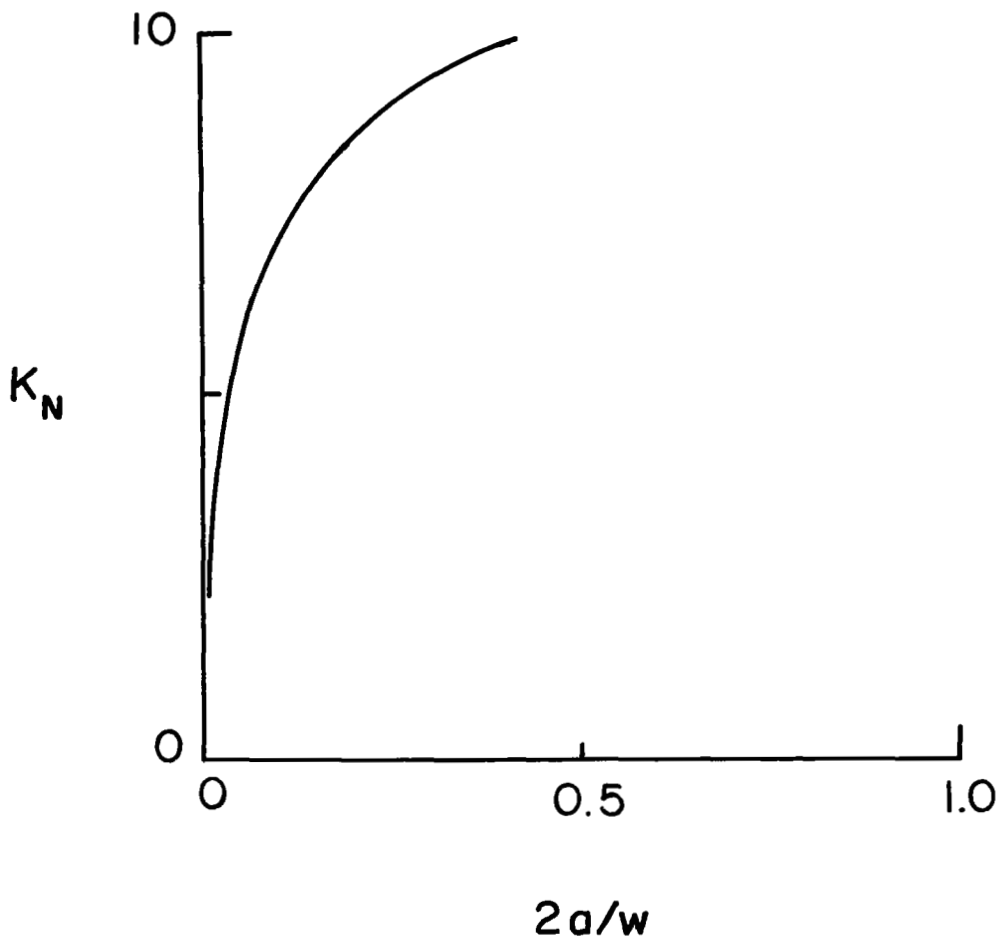

Figure 2.- Variation of K_N with 2a/w for a 2-inch-wide (51-mm) sheet specimen made of 7075-T6 aluminum alloy.

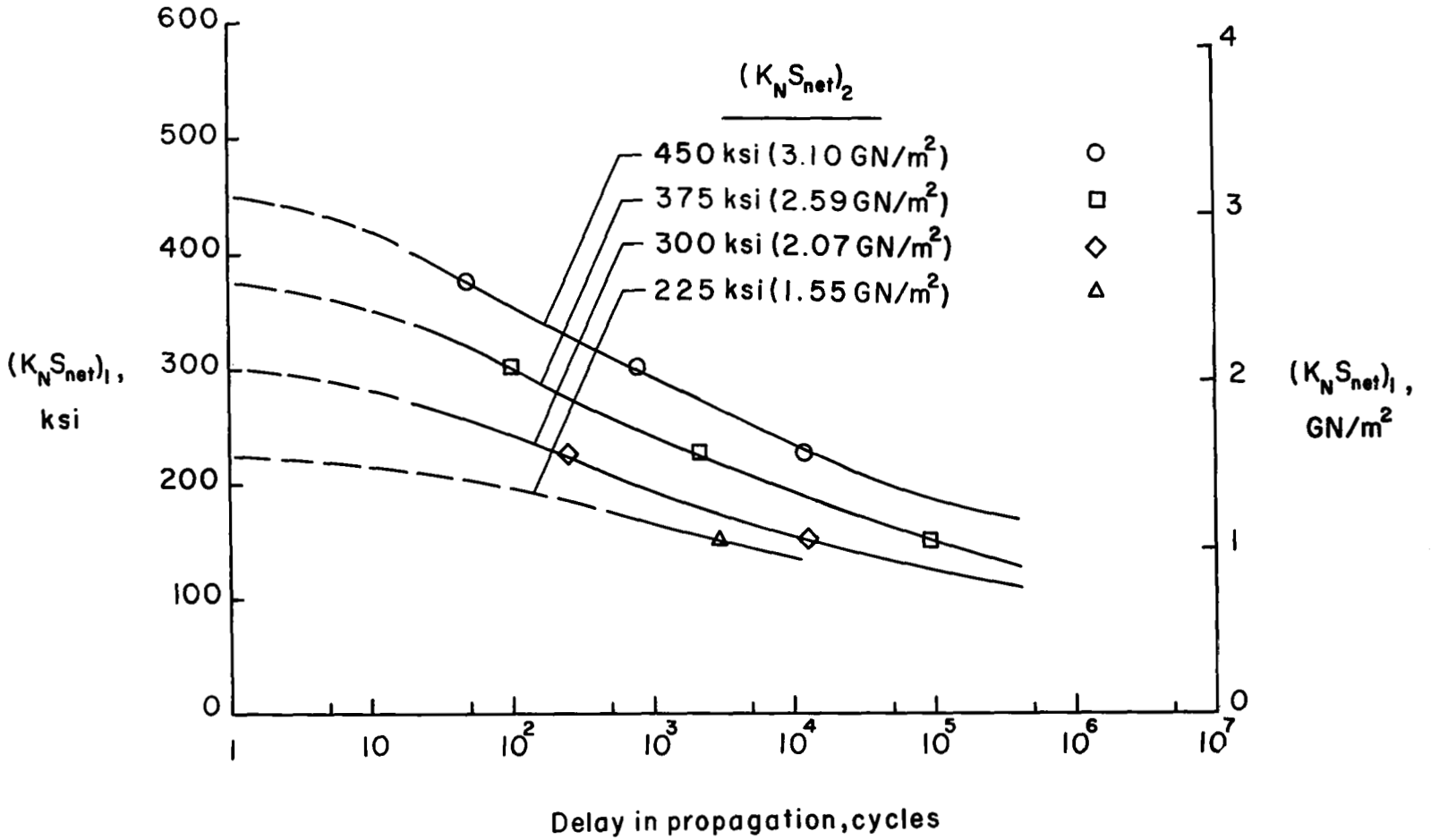

Figure 3.- Delay in propagation resulting from a single prior high-load cycle. Test series I.

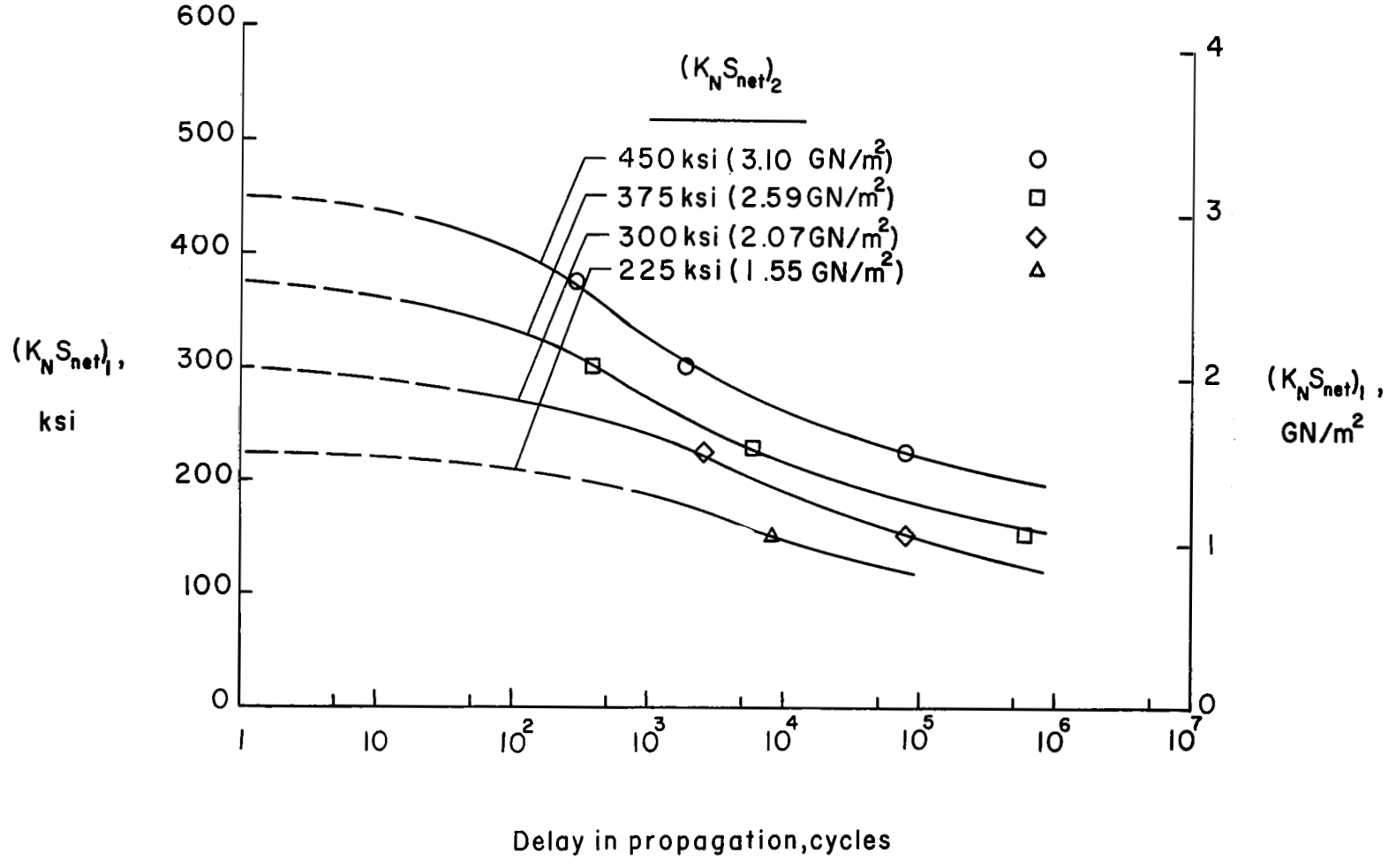

Figure 4.- Delay in propagation resulting from multiple prior high-load cycles. Test series II.

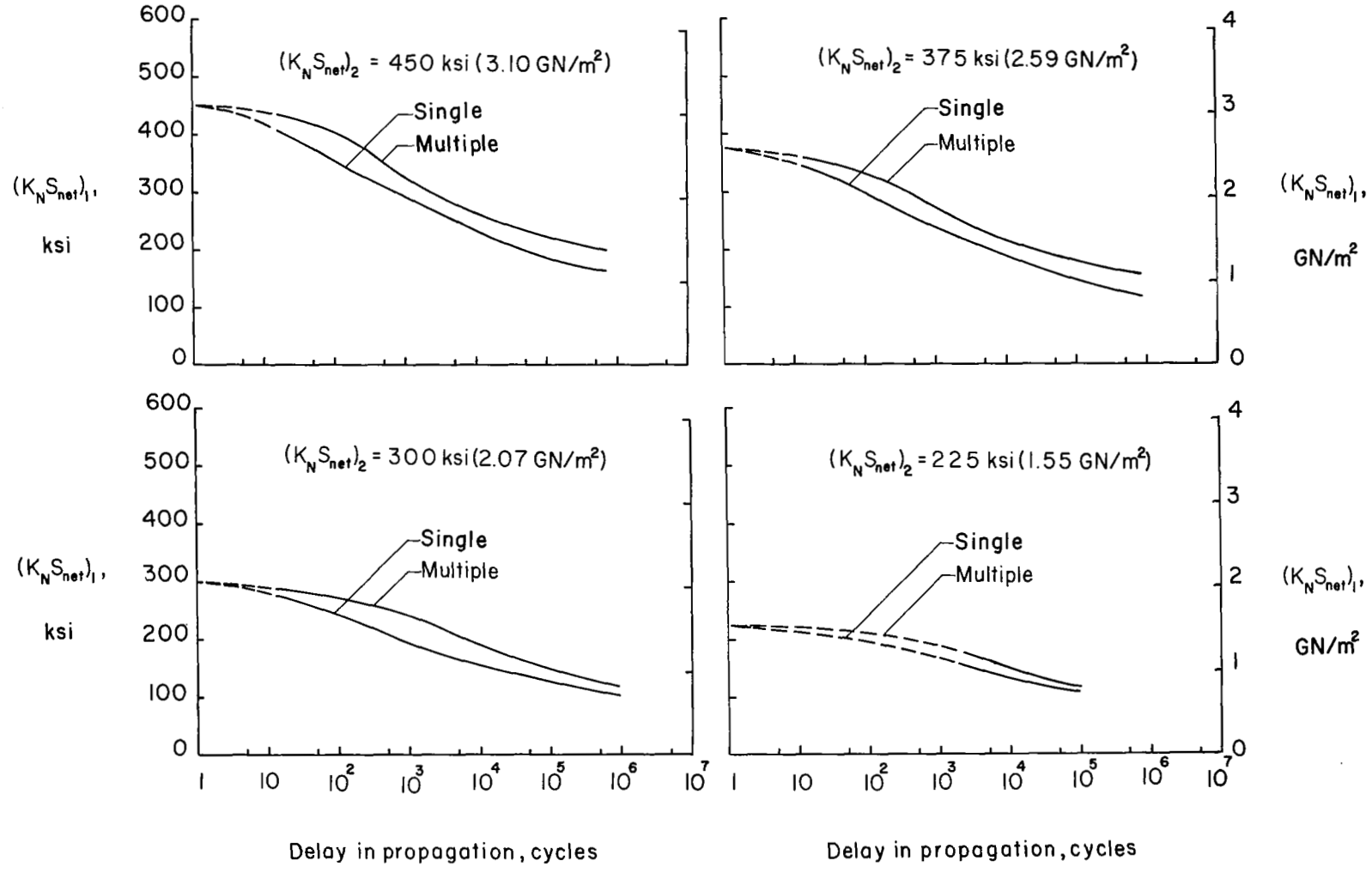

Figure 5.- Comparison of delays in propagation resulting from single and multiple high-load cycles.

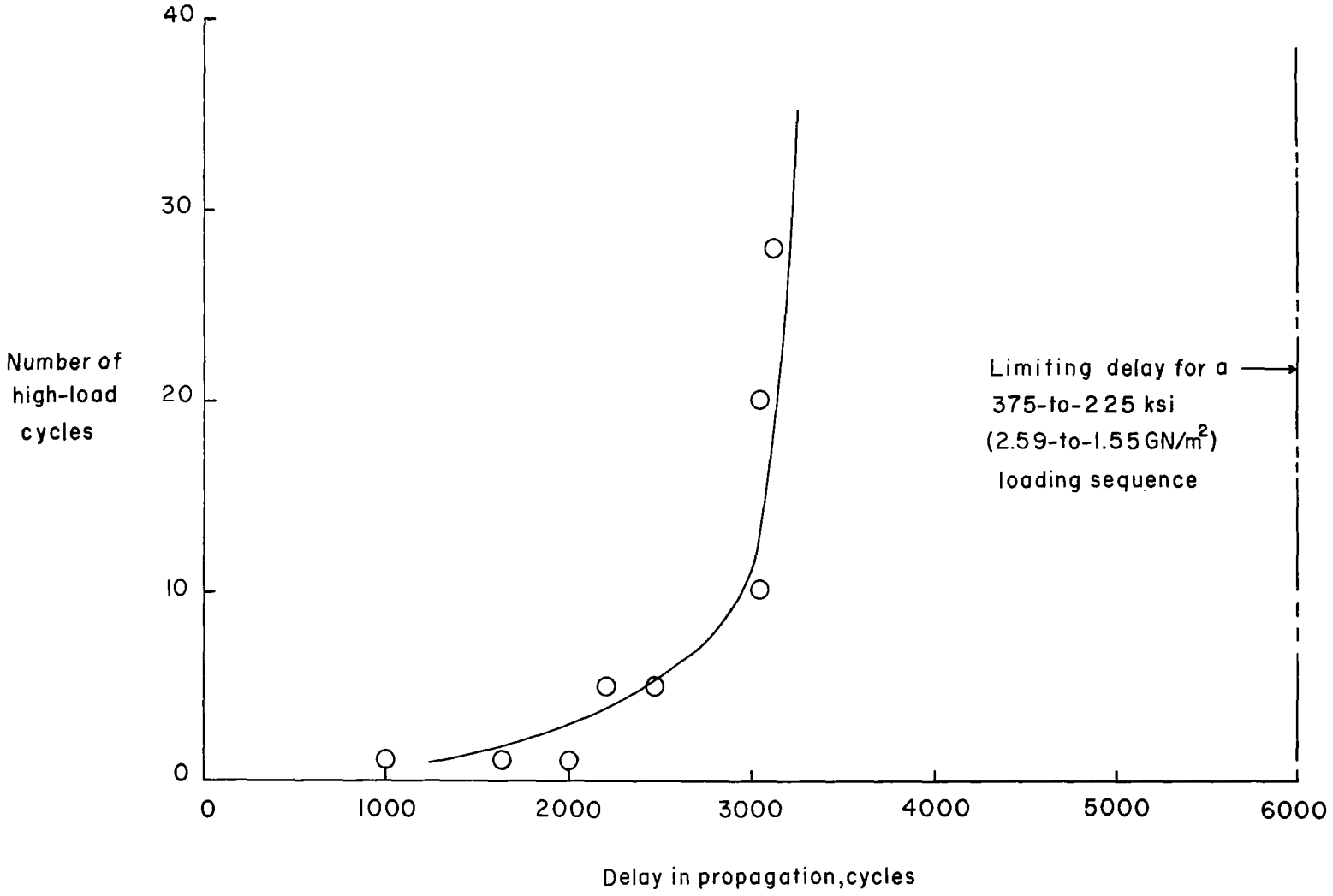

Figure 6.- Variation of delay in propagation with number of high-load cycles in test series III.

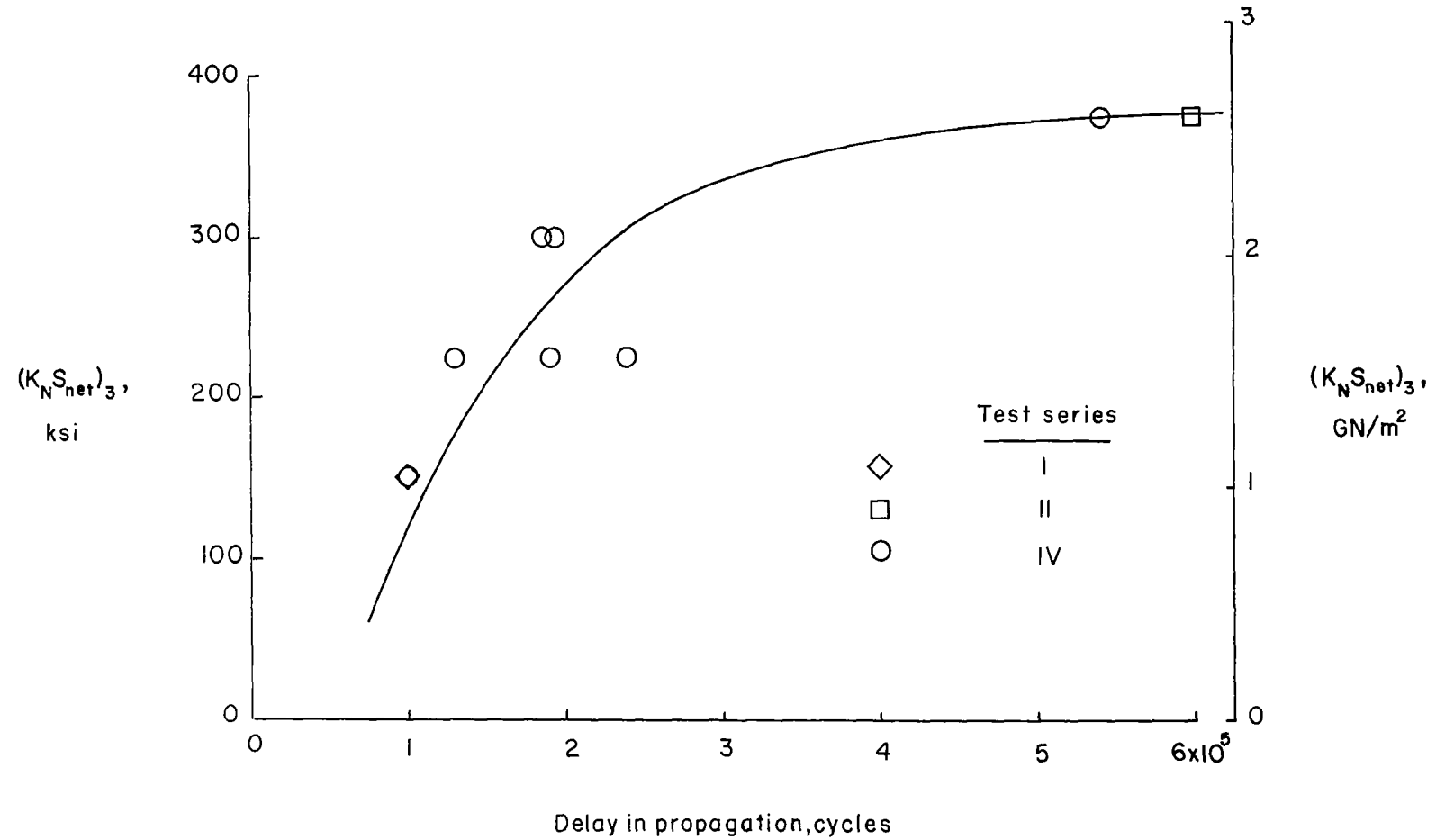

Figure 7.- Variation of delay in propagation with $(K_N S_{net})_3$ in test series IV.

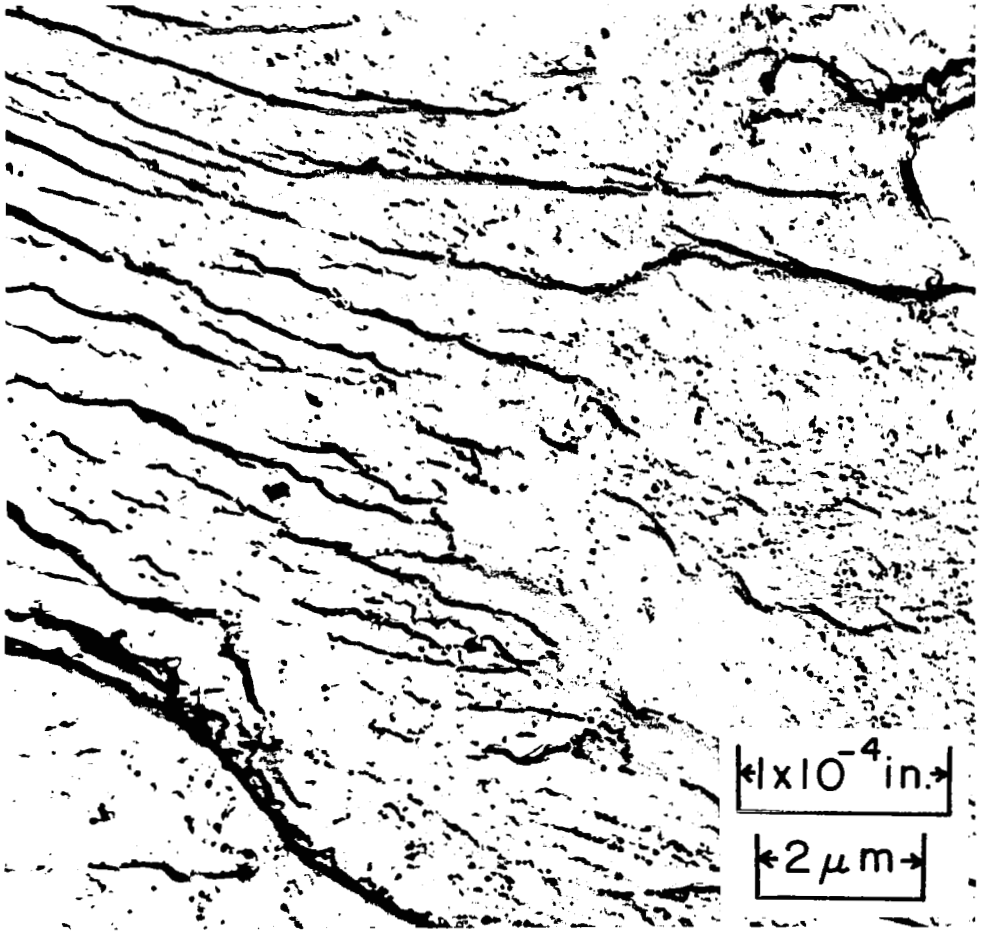

L-70-1501

(a) Fatigue striations resulting from $K_N S_{net}$ = 150 ksi $(1.03\ GN/m^2)$ cycles applied immediately before the $K_N S_{net}$ = 375 ksi $(2.59\ GN/m^2)$ cycle.

Figure 8.- Electron-fractograph of specimen from test series I at $K_N S_{net}$ values of 150, 375, and 150 ksi $(1.03, 2.59, \text{and } 1.03\ GN/m^2)$.

L-70-1502

(b) Fatigue striations resulting from $K_N S_{net}$ = 150 ksi $\left(1.03\ GN/m^2\right)$ cycles applied immediately after the $K_N S_{net}$ = 375 ksi $\left(2.59\ GN/m^2\right)$ cycle.

Figure 8.- Concluded.

NASA-Langley, 1970 —— 17 L-6834